Nonlinear Dynamic Behaviour of The Mechanisms Having Clearance and Compliant Joints

Amir Hossein Javanfar*
Department of Mechanical Engineering,
Shahrood University of Technology, Iran
E-mail: Amirhosein.javanfar@yahoo.com
*Corresponding author

Abstract: In this paper, the rigid four-bar linkage with clearance joint has been examined. The effects of design parameters have been analyzed separately. Considering chaotic behaviour and undesirable vibrations of the system induced by joint clearance, it has been suggested to use compliant joints for improving these undesirable behaviours. Therefore, rigid four-bar linkage with clearance joint and compliant joint is investigated by pseudo-rigid-body model. Subsequently, the nonlinear behaviour of the compliant mechanism is examined, using fast Fourier transform analysis, Poincare sections, and bifurcation diagram. Comparative analysis of results clearly shows that using appropriate compliant joints causes notable improvements in the behaviour of the system, reduction of sudden impacts, and lower accelerations. 6 cycles simulations of mechanisms demonstrate the decreasing 207 impacts to 33 impacts using compliant joint. Moreover, the results report 87% decrease in follower top acceleration and 64% in clearance joint top contact force. Although using the compliant joint makes limitations in the workspace, but the appropriate and optimized design of the compliant joint results in good improvement in the performance of the system.

Biographical notes: Amir Hossein Javanfar received his MSc in Mechanical Engineering from Babol Noshirvani University of Technology in 2015. He is currently a student at the Mechanical Engineering, Shahrood University of Technology, Shahrood, Iran. His current research interest includes contact mechanics and nonlinear dynamics.

Research paper

1   INTRODUCTION

The existence of joint clearance results in additional degrees of freedom in the system and the mechanism undergoes sudden impacts, causing undesirable vibrations, lower accuracy, and chaotic dynamical behaviour [1]. Therefore, by considering joint clearance in mechanisms analysis, more accurate information can be obtained and a better design of mechanism can be achieved. Clearance phenomenon in joint causes three modes of relative motion for journal and bearing: (i) free flight mode, (ii) impact mode, and (iii) continuous contact mode [2]. The massless link model [2] is unable to predict these three modes, so to achieve more accurate responses; a more perfect model is required for dynamical analysis.

While ignoring the energy dissipation [3] results in a great error in the response and reduces the accuracy, the model developed by Lankarani and Nikravesh [4] presented a hysteresis damping function in order to account for the dissipated energy during contact, and all motional modes are assumed. The computational and experimental study [5-6] on revolute clearance joints is developed for improving the accuracy of modeling and using the model in applicable cases [7-9]. Respecting the importance of clearance modeling in mechanisms, Lankarani and Nikravesh model is used in [10] to present the nonlinear dynamics of the four-bar linkage mechanism with two clearance joints. Moreover, the perfect contact model should consider other phenomena like friction and lubrication. Javanfar and Bamdad [11] presented a novel friction model for clearance joint modeling to reduce the error of these models. Filipe Marques et al. [12] examined several friction force models for improving the accuracy of clearance joint modeling.

As the researches and studies have been improved in the field of clearance joints, special and practical works have been done in dynamic analysis, control, and design of mechanisms [13-20] to reduce undesirable vibration of mechanisms with clearance joints. Studies [13-14] demonstrate the chaotic behaviour of these mechanisms, then the journal-bearing motion is stabilized by a control method [13-14]. Using the genetic algorithm, the appropriate values for variables design parameters are determined in order to reduce undesirable system vibrations [15]. However, the permanent contact model is assumed in [15]. Sardashti et. al. [16] designed a rigid planar four-bar linkage mechanism with clearance joints via PSO algorithm that uses the massless link method. Although, they [15-16] applied optimization method for reducing vibration of mechanisms with clearance joint, but their modeling is not accurate. Therefore, considering all motional modes in the clearance joint optimal design is used to remove impact in the clearance joint [17]. Some practical examples relate the closed-

chain mechanism dynamics to the necessity of the joint clearance model [18-20]. Although mentioned papers [13-20] used optimization and control methods in the field of improving the dynamic behaviour of these mechanisms, some studies using stiffness and flexibility reduce the undesirable vibration of clearance joint in mechanisms [21-22]. They report that the flexibility and stiffness of the linkages [21] and joints [22] can improve these mechanisms' behaviour. Because of limitations and the high cost of optimization and control methods, concentrating on the compliant joint for this goal is efficient. Bending compliant joint is one of the flexible links that has been noted because of their vast utility such as MEMS, robotics, medical usage, and biomechanics application [23].

Studies [22-24], support the idea of adding compliant joints to the mechanisms with clearance for improving accuracy and reducing vibration, while they [22-24] do not consider the nonlinear behaviour by Poincare section, phase diagram, and FFT plot. Studies [21], [25] suggest the link flexibility and passive vibration absorber to improve the chaotic behaviour of the mechanism considering nonlinear behaviour. Although studies [21], [25] apply the link flexibility and passive vibration absorber to improve nonlinear behaviour, they do not use compliant joint, and studies [22], [24] apply compliant joint to improve the dynamic behaviour of the mechanism but do not present the nonlinear behaviour. Therefore, in the present work, it is simply shown how sudden impacts in the system are eliminated, undesirable vibrations are decreased and chaotic behaviour is improved using a compliant joint.

Although joint clearance has been gaining increasing attention in recent years, most works have been devoted to analyzing and controlling undesirable system vibrations, and despite many studies have been carried out in the area of compliant joints, simultaneous effect of both in one mechanism and nonlinear behaviour of them have never been addressed. Therefore, the analysis of the mechanism predicts the influence of compliant joint on the nonlinear dynamic behaviour of mechanisms with clearance joint. The contribution of this paper is:

• Offering and examining a compliant joint to predict the effect of the compliant joint on the behaviour of mechanisms with clearance joint.

• Presenting the nonlinear behaviour of four-bar linkage mechanism with clearance and compliant joint by Poincare section, phase diagram, and FFT plot.

The rest of the paper is structured as follows. The mechanism's model is presented, and the stiffness of the compliant joint is introduced in Section 2. Then, results show the influence of compliant joint on the dynamic behaviour of mechanism with clearance joint in section 3. The results including journal center trajectory and input link required moment and concentrating on the vibrations of mechanisms, nonlinear dynamics plots as

the phase diagram, Poincare section, FFT analysis, and bifurcation diagram are presented.

2   MODELING

In this section Equations of motions for different cases are obtained. "Fig. 1" shows the schematic of the clearance joint that demonstrates the contact point P_B and P_j, the center of journal O_j, the center of bearing O_B, the clearance vector r and α.
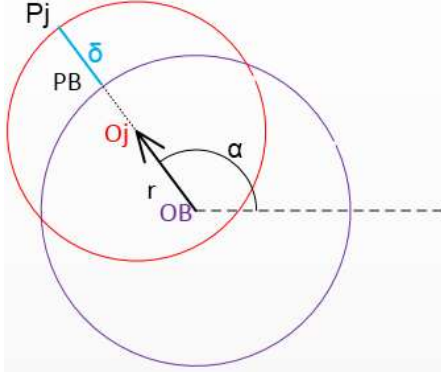
Fig. 1   Revolute clearance joint.

R_j and R_B are the radius of journal and bearing, hence indentation δ is calculated as:

$$\delta = r - (R_B - R_j) \tag{1}$$

The Hertz law as proposed in [3]:

$$F_N = K\delta^n \tag{2}$$

Assuming circular and elliptical contacts n is set to 1.5. The generalized stiffness K is written as:

$$K = \frac{4}{3(\sigma_i + \sigma_j)}\left(\frac{R_i R_j}{R_i + R_j}\right)^{\frac{1}{2}} \tag{3}$$

σ_i and σ_j are material parameters. The values of them are calculated by using Poisson's ratio υ and the Young's modulus E of each sphere as follows:

$$\sigma_k = \frac{1 - \upsilon_k^2}{E_k}, \quad k = i,j \tag{4}$$

The normal contact force is finally expressed as [4]:

$$F_N = K\delta^n\left(1 + \frac{3k(1 - C_e^2)}{4\dot{\delta}^{(-)}}\right)\frac{\dot{\delta}}{\dot{\delta}^{(-)}} \tag{5}$$

For sphere to sphere contact or by similar expressions for the contact of other types of geometry; C_e is the restitution coefficient and $\dot{\delta}^{(-)}$ is the initial normal impact velocity where contact is detected. Note that the direction of normal force is the same with the normal vector (n) in "Fig. 2". The contact force magnitude Q_c and its orientation α are defined contact force vector and Q_c is computed as:

$$Q_c = K\delta^{1.5}\left(1 + \frac{3(1 - c_e^2)}{4}\frac{\dot{r}}{\dot{r}^{(-)}}\right) \tag{6}$$
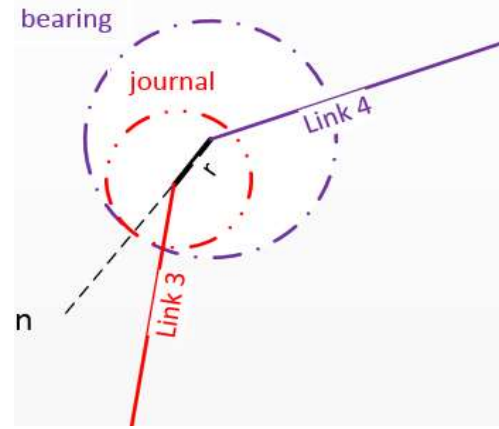
Fig. 2   Equivalent clearance link.

A brief review of compliant joints and their application are presented here. In order to design compliant joint, some criteria should be noted like: (i) range of motion, (ii) stress concentration (iii) axial stiffness. Using these studies of designing [26-28] and investigating [29-30] the revolute joint and the translational compliant joint are applied. The revolute compliant joint which is a bending element, is supposed as a torsional spring, whose stiffness can be calculated by using the Castigliano's theory [30]. According to this theory, the torsional spring coefficient of compliant joint according to "Fig. 3" is calculated as [31]:

$$K = \frac{EI}{L} = \frac{EI}{2R\Delta\theta} \tag{10}$$

Where, L is the length of the flexible segment, E is elasticity modulus, I is moment inertia and R is beam curvature radius.

The EoM (Equation of motion) for the mechanism of "Fig. 4" is derived. It is assumed that joints have clearance. Three cases are considered: (1) one clearance joint, (b) one clearance and compliant joint, and (c) one and two compliant joints. Moreover, the Euler-Lagrange Equation is used to extract the EoM. Figure 4 shows the

mechanism with one clearance joint at joint 3 having the 3 degrees of freedom.
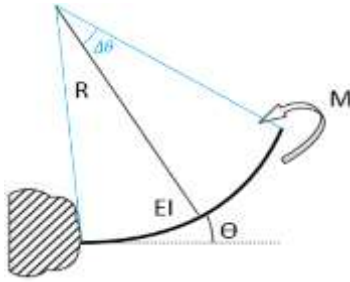
Fig. 3   Compliant joint.
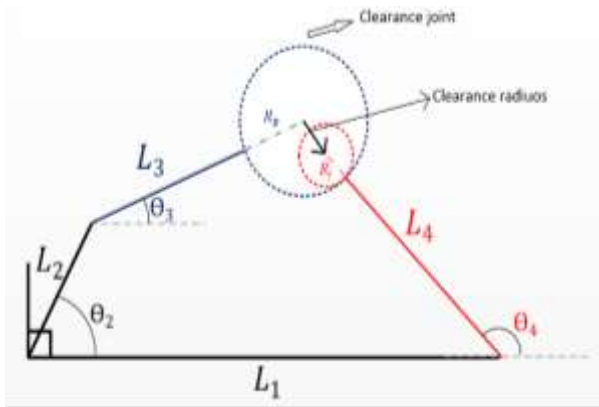
Fig. 4   Four bar linkage mechanism with one clearance joint.

The Equations of motion for this system is as follows:

$$
\begin{aligned}
(I_3 + m_3 a_3^2 L_3^2)\ddot{\theta}_3 - m_3 a_3 L_3 L_2 \dot{\theta}_2^2 \cos(\theta_2 \\
- \theta_3 - \lambda_3) \\
+ m_3 a_3 L_3 \mathrm{g}\cos(\theta_3 + \lambda_3) \\
= -L_3 Q_c \sin(\theta_3 - \psi)
\end{aligned} \tag{11}
$$

$$
\begin{aligned}
(I_4 + m_4 a_4^2 L_4^2)\ddot{\theta}_4 + m_4 a_4 L_4 \mathrm{g}\cos(\theta_4 + \lambda_4) \\
= Q_c L_4 \sin(\theta_4 - \psi)
\end{aligned} \tag{12}
$$

The required moment to drive the crank is obtained as:

$$
\begin{aligned}
\big(I_2 + m_2 a_2^2 L_2^2 + m_3 L_2^2 \\
+ m_3 a_3 L_3 L_2 \dot{\theta}_3 \cos(\theta_2 \\
- \theta_3)\big)\ddot{\theta}_2 \\
+ m_3 a_3 L_3 L_2 \dot{\theta}_2 \big(\ddot{\theta}_3 \cos(\theta_2 \\
- \theta_3) - (\dot{\theta}_2 \\
- \dot{\theta}_3)\sin(\theta_2 - \theta_3)\dot{\theta}_3\big) \\
- m_3 a_3 L_3 L_2 \dot{\theta}_2 \dot{\theta}_3 \sin(\theta_2 \\
- \theta_3) + m_2 \mathrm{g} a_2 L_2 \cos\theta_2 \\
+ m_3 \mathrm{g} L_2 \cos\theta_2 \\
+ Q_c L_2 \sin(\theta_2 - \psi) = M
\end{aligned} \tag{13}
$$

The schematic of the mechanism adding a compliant joint to case (i) is demonstrated in "Fig. 5". Joint 2 is compliant, while joint 3 is clearance joint.
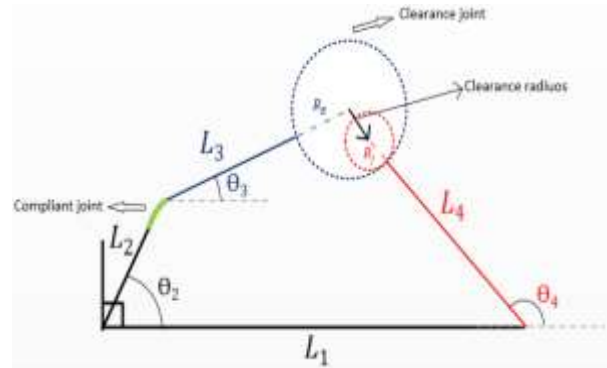
Fig. 5   Four bar linkage mechanism with one clearance joint and one compliant joint.

As mentioned in modeling section, compliant joint modeled as torsional spring, so four-bar linkage mechanism via pseudo-rigid-body model is demonstrated by "Fig. 6".
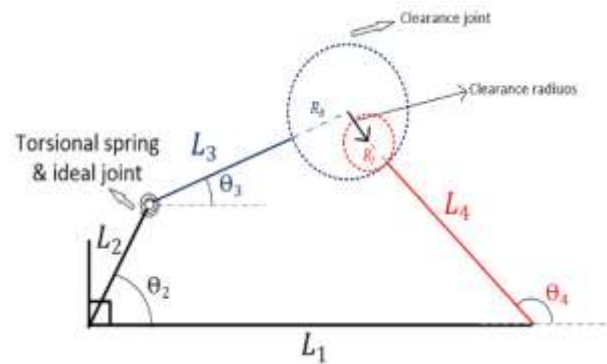
Fig. 6   Modeling of four bar linkage mechanism with one clearance joint and one compliant joint according pseudo-rigid-body model.

According pseudo-rigid-body model of compliant mechanisms, the Equations of motion for this case can be expressed by following Equations.

$$
\begin{aligned}
(I_3 + m_3 a_3^2 L_3^2)\ddot{\theta}_3 \\
- m_3 a_3 L_3 L_2 \dot{\theta}_2^2 \cos(\theta_2 \\
- \theta_3 - \lambda_3) \\
+ m_3 a_3 L_3 g \cos(\theta_3 + \lambda_3) \\
- k_\theta(\theta_2 - \theta_3) \\
= -L_3 Q_c \sin(\theta_3 - \psi)
\end{aligned} \tag{15}
$$

$$
\begin{aligned}
(I_4 + m_4 a_4^2 L_4^2)\ddot{\theta}_4 + m_4 a_4 L_4 \mathrm{g}\cos(\theta_4 + \lambda_4) \\
= Q_c L_4 \sin(\theta_4 - \psi)
\end{aligned} \tag{16}
$$

The required moment driving the crank is written as:

$$
\begin{aligned}
\big(I_2 + m_2 a_2^2 L_2^2 + m_3 L_2^2 \\
+ m_3 a_3 L_3 L_2 \dot\theta_3 \cos(\theta_2 \\
- \theta_3)\big)\ddot\theta_2 \\
+ m_3 a_3 L_3 L_2 \dot\theta_2 \big(\ddot\theta_3 \cos(\theta_2 \\
- \theta_3) - \big(\dot\theta_2 \\
- \dot\theta_3\big)\sin(\theta_2 - \theta_3)\,\dot\theta_3\big) \\
- m_3 a_3 L_3 L_2 \dot\theta_2 \dot\theta_3 \sin(\theta_2 \\
- \theta_3) + m_2 g a_2 L_2 \cos\theta_2 \\
+ m_3 g L_2 \cos\theta_2 \\
+ Q_c L_2 \sin(\theta_2 - \psi) \\
+ K_\theta\big(\theta_2 - \theta_3 \\
- (\theta_{20} - \theta_{30})\big) = M_2
\end{aligned}
\tag{17}
$$

The Eom of mechanism with compliant joints is presented here. In this case, similar to a four-bar mechanism without clearance, the mechanism has a single degree of freedom (DoF). The kinematics solution of the system is the same as the case with ideal joints, however, the required crank moment is different. Figure 7 demonstrates the mechanism with two compliant joints. Compliant joint was modeled as torsional spring, so four-bar linkage mechanism via this modeling demonstrated by "Fig. 8".
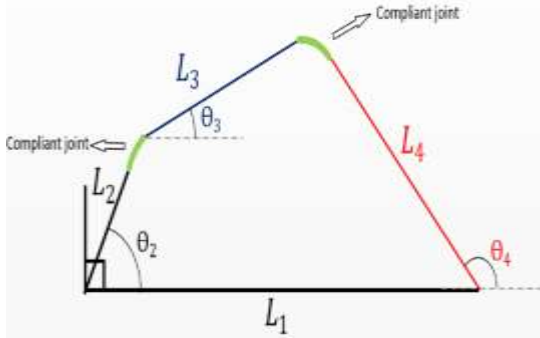
Fig. 7   Four bar linkage mechanism with two compliant joint.
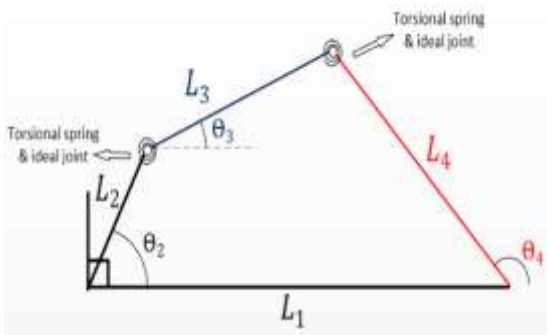
Fig. 8   Modeling of four bar linkage mechanism with two compliant joint

Using kinematic solution of mechanism, the value of kinematic specification of mechanism's links are obtained, so the crank moment of mechanism is calculated by using these values. These values are calculated as:

$$
L_2 e^{i\theta_2} + L_3 e^{i\theta_3} = L_1 e^{i\theta_1} + L_4 e^{i\theta_4}
\tag{15}
$$

$$
\begin{aligned}
\ddot\theta_3 &= -\frac{L_2}{L_3}\Bigg[\ddot\theta_2 \frac{\sin(\theta_2 - \theta_4)}{\sin(\theta_3 - \theta_4)} \\
&+ \dot\theta_2(\dot\theta_2 - \dot\theta_4)\frac{\cos(\theta_2 - \theta_4)}{\sin(\theta_3 - \theta_4)} \\
&- \dot\theta_2(\dot\theta_3 - \dot\theta_4)\frac{\cos(\theta_2 - \theta_4)\cos(\theta_3 - \theta_4)}{\sin^2(\theta_3 - \theta_4)}\Bigg]
\end{aligned}
\tag{16}
$$

$$
\begin{aligned}
\ddot\theta_4 &= \frac{L_2}{L_4}\Bigg[\ddot\theta_2 \frac{\sin(\theta_2 - \theta_3)}{\sin(\theta_4 - \theta_3)} \\
&+ \dot\theta_2(\dot\theta_2 - \dot\theta_3)\frac{\cos(\theta_2 - \theta_3)}{\sin(\theta_4 - \theta_3)} \\
&- \dot\theta_2(\dot\theta_4 - \dot\theta_3)\frac{\sin(\theta_2 - \theta_3)\cos(\theta_4 - \theta_3)}{\sin^2(\theta_4 - \theta_3)}\Bigg]
\end{aligned}
\tag{17}
$$

Moreover, in this case the input crank moment is determined as:

$$
\begin{aligned}
&\Bigg[I_{G_2} + m_2 \frac{L_2^2}{4} + m_3 L_2^2 \\
&+ \left(\frac{L_2}{L_3}\right)^2 \left(I_{G_3} + m_3 \frac{L_3^2}{4}\right)\left(\frac{\sin(\theta_2 - \theta_4)}{\sin(\theta_3 - \theta_4)}\right)^2 \\
&- m_3 L_2^2 \cos(\theta_3 - \theta_2)\frac{\sin(\theta_2 - \theta_4)}{\sin(\theta_3 - \theta_4)} \\
&+ \left(I_{G_4} + m_4 \frac{L_4^2}{4}\right)\left(\frac{L_2}{L_4}\right)^2 \left(\frac{\sin(\theta_2 - \theta_3)}{\sin(\theta_4 - \theta_3)}\right)^2\Bigg]\ddot\theta_2 \\
&+ \Bigg[2\left(\frac{L_2}{L_3}\right)^2 \bigg(I_{G_3} \\
&+ m_3 \frac{L_3^2}{4}\bigg)\frac{\sin(\theta_2 - \theta_4)}{\sin^2(\theta_3 - \theta_4)}\bigg(\cos(\theta_2 - \theta_4)\,(\dot\theta_2 \\
&- \dot\theta_4) \\
&- \frac{\sin(\theta_2 - \theta_4)\cos(\theta_3 - \theta_4)}{\sin(\theta_3 - \theta_4)}(\dot\theta_3 - \dot\theta_4)\bigg) \\
&+ m_3 L_2^2 \sin(\theta_3 - \theta_2)\frac{\sin(\theta_2 - \theta_4)}{\sin(\theta_3 - \theta_4)}(\dot\theta_3 - \dot\theta_2)
\end{aligned}
\tag{18}
$$

$$-m_3 L_2^2 \cos(\theta_3 - \theta_2) \left[\frac{\cos(\theta_2 - \theta_4)}{\sin(\theta_3 - \theta_4)} (\dot{\theta}_2 - \dot{\theta}_4) \right.$$
$$- \sin(\theta_2$$
$$\left. - \theta_4) \frac{\cos(\theta_3 - \theta_4)}{\sin^2(\theta_3 - \theta_4)} (\dot{\theta}_3 \right.$$
$$\left. - \dot{\theta}_4) \right]$$

$$+2 \left(I_{G_4} \right.$$
$$+ m_4 \frac{L_4^2}{4} \right) \left(\frac{L_2}{L_4} \right)^2 \frac{\sin(\theta_2 - \theta_3)}{\sin(\theta_4 - \theta_3)} \left(\frac{(\dot{\theta}_2 - \dot{\theta}_3) \cos(\theta_?}{\sin(\theta_4 - \theta_?)} \right.$$
$$\left. - \frac{(\dot{\theta}_4 - \dot{\theta}_3) \cos(\theta_4 - \theta_3) \sin(\theta_2 - \theta_3)}{\sin^2(\theta_4 - \theta_3)} \right) \right] \dot{\theta}_2$$
$$- \frac{1}{2} m_3 L_2 L_3 \dot{\theta}_2 \dot{\theta}_3 \sin(\theta_3 - \theta_2)$$
$$+ m_2 g a_2 L_2 \cos\theta_2 + m_3 g L_2 \cos\theta_2$$
$$+ m_3 g L_{G_3} \frac{L_2}{L_3} \frac{\sin(\theta_2 - \theta_4)}{\sin(\theta_3 - \theta_4)} \sin\theta_3$$
$$+ m_4 g L_{G4} \frac{L_2}{L_4} \frac{\sin(\theta_2 - \theta_3)}{\sin(\theta_4 - \theta_3)} \cos\theta_4$$
$$+ \left(1 + \frac{L_2}{L_3} \frac{\sin(\theta_2 - \theta_4)}{\sin(\theta_3 - \theta_4)} \right) K_{\Theta_1} (\theta_2 - \theta_3$$
$$- (\theta_{20} - \theta_{30}))$$
$$- \left(\frac{L_2}{L_3} \frac{\sin(\theta_2 - \theta_4)}{\sin(\theta_3 - \theta_4)} \right.$$
$$\left. + \frac{L_2}{L_4} \frac{\sin(\theta_2 - \theta_3)}{\sin(\theta_4 - \theta_3)} \right) K_{\Theta_2} (\theta_3$$
$$- \theta_4 - (\theta_{30} - \theta_{40})) = M$$

Where K_{Θ_1} and K_{Θ_2} are torsional stiffness coefficient of joints 2 and 3. The Equation of mechanism with one compliant joint can be achieved considering $K_{\Theta_2} = 0$.

3   RESULTS AND DISCUSSION

The influence of the compliant joints on the dynamic results of mechanism is investigated. The variable angular displacement of crank is:

$$\theta_2 = \Theta \cos \omega t + \theta_{0_2} \tag{19}$$

Where, Θ and θ_{0_2} are the amplitude of oscillation and initial configuration. Mass and geometric properties of links are mentioned in "Table 1". Properties of the journal and bearing are mentioned in "Table 2". It is clear that the compliant joint cannot have complete rotation, hence crank must has oscillation. For

considered mechanism, Θ and θ_{0_2} are selected as $\frac{441\pi}{180}$ and 2.1, respectively. And "Table 3", shows the specifications of the compliant joint.

Table 1 The specification of different links.

Body number	Length (m)	Mass (kg)	a
1	0.08	-	0.5
2	0.01	1.405	0.5
3	0.075	7.866	0.5
4	0.055	6.407	0.5

Table 2 Geometrical and structural properties of journal and bearing.

Bearing radius	Clearance size	Restitution coefficient	Young's modulus	Poisson's ratio
0.001	0.0005	0.9	207 (Gpa)	0.5

Table 3 The specification of compliant joint.

Modulus of elasticity	$E = 207 \times 10^9 pa$
Radius of curvature	R=0.1981m
widths	W=0.01m
thickness	t=0.001m
joint stiffness	K=4.05

In "Fig. 9", the time histories of the magnitude of the clearance vector are demonstrated. It is obvious that the joint experiences three motional modes. However, in continuous contact mode, the dynamic behaviour of the system is improved, so based on this concept, compliant joint is applied in order to have journal and bearing experience continuous contact mode more than the case that mechanism without compliant joint. Actually, "Fig. 9", shows the clearance trajectory for several stiffnesses of compliant joints, also this figure demonstrates that using proportional stiffness of compliant joint stabilizes the clearance joint in continuous contact mode. Moreover, "Fig. 9b" confirms that using compliant joint impact and free flight mode are decreased. Generally, this figure proves the idea that using proportional compliant joint increases the continuous contact mode. Moreover, the advantage of these figures allowed the investigation of using compliant joints in order to eliminate the undesirable vibration of the mechanism. The influence of clearance size and input link velocity are investigated separately, therefore "Fig. 10" demonstrates the journal center trajectory relative to bearing in several input link velocities, and "Fig. 11" shows the variation of clearance with time in several input link velocities.
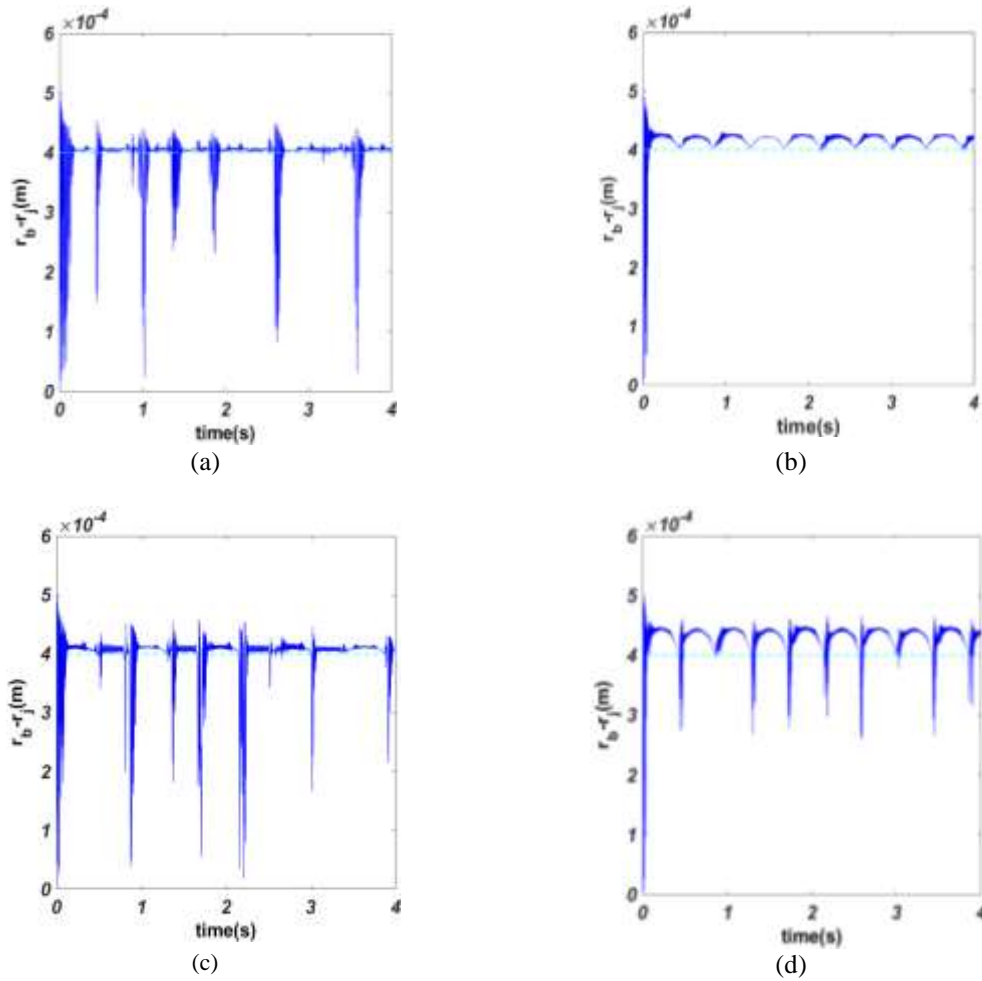
Fig. 9   Variation of clearance with time: (a): four bar linkage mechanism with one clearance joint at joint 3, and four bar linkage
mechanism with one clearance joint at joint 3 and compliant joint at joint 2 with stiffness of, (b): 4 N.m, (c): 1 N.m, (d): 10 N.m.
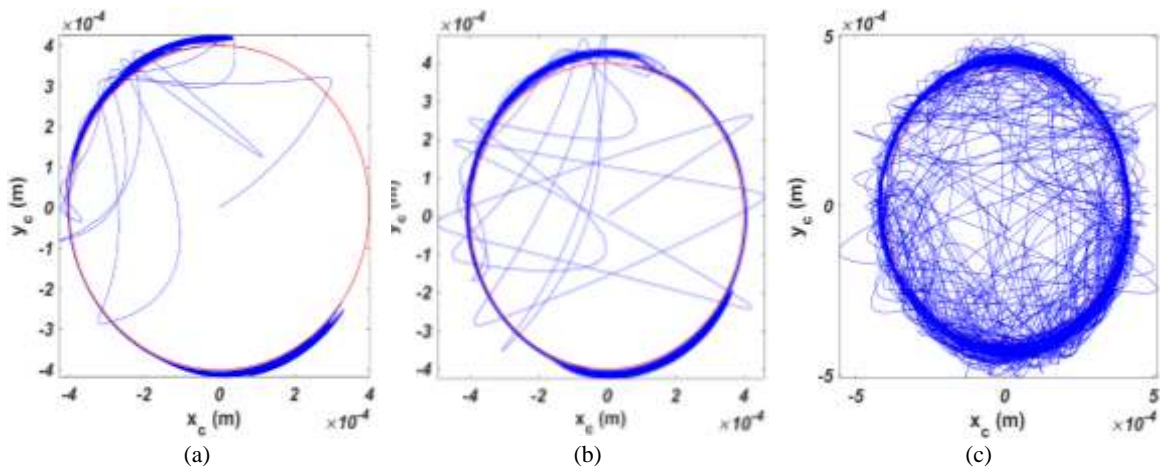
Fig. 10   Journal center trajectory relative to bearing (red circle shows the clearance size) with input link velocity:
(a): 20 rpm, (b): 70 rpm, (c): 150 rpm.
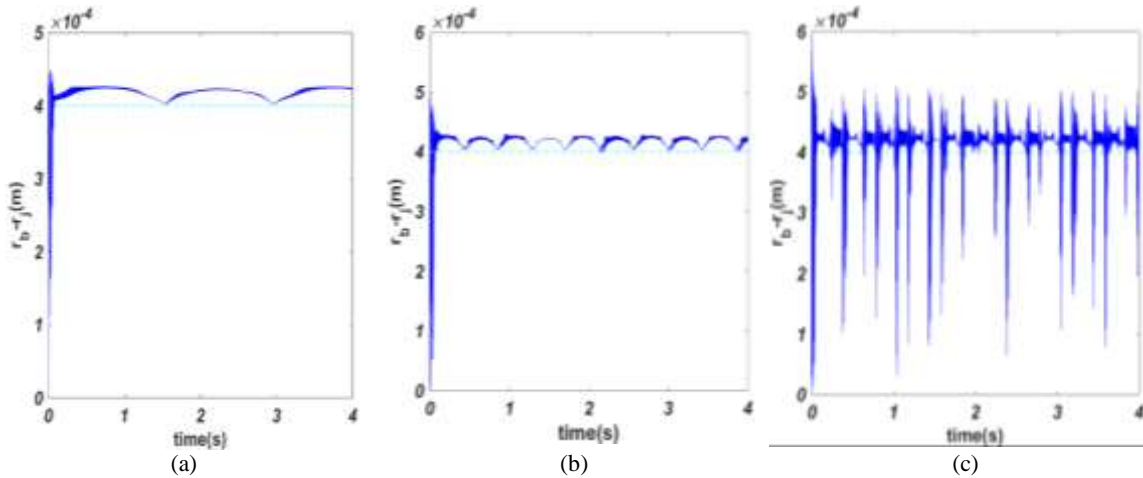
Fig. 11   Variation of clearance with time with input link velocity: (a): 20 rpm, (b): 70 rpm, (c): 150 rpm.

Figure 12 demonstrates the Journal center trajectory relative to bearing in several clearance sizes and "Fig. 13" shows the variation of clearance with time in several clearance sizes. Actually based on physical concepts increasing these parameters is undesirable. Also, the advantage of these figures verifies that increasing clearance size and input link, velocity is not desirable in fact, increasing these parameters causes more impact and major clearance radius.
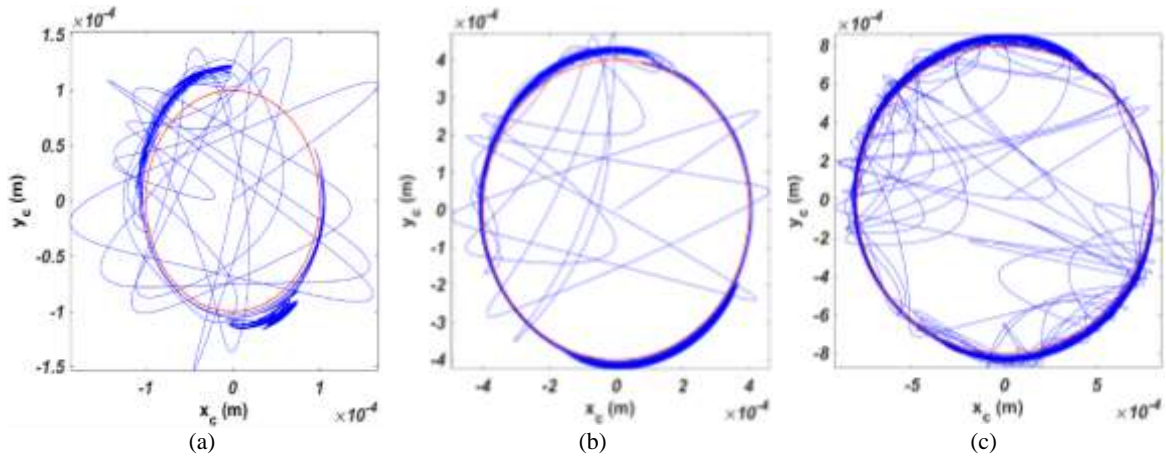
Fig. 12   Journal center trajectory relative to bearing (red circle shows the clearance size) with clearance size of: (a): 0.0001 m, (b): 0.0004 m (c) 0.0008 m.
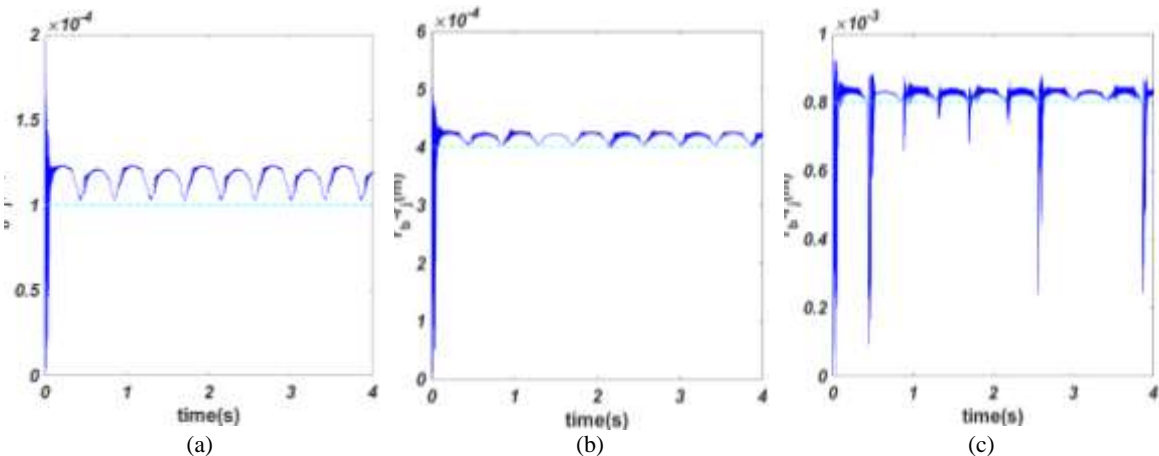
Fig. 13   Variation of clearance with time with clearance size of: (a): 0.0001 m, (b): 0.0004 m (c) 0.0008 m.

Figures 14 and 15 give the required moment of driving input link for the case of mechanism with clearance joint and with compliant joint. It is obvious when the angular velocity and clearance size are increased, the vibration of the mechanism is increased.
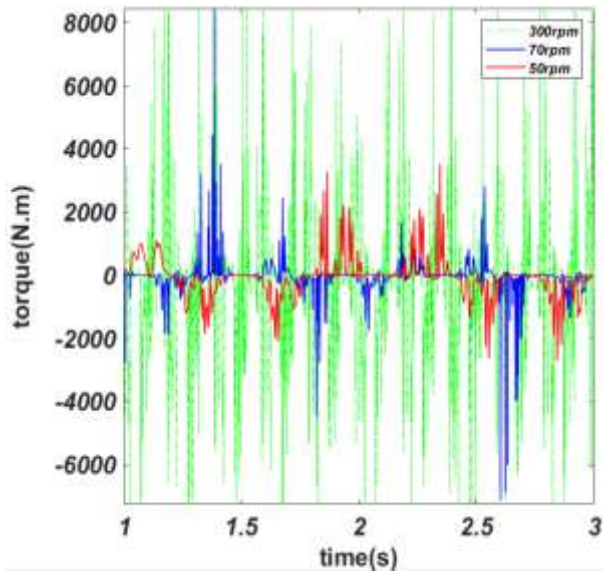
Fig. 14   Crank moment for different angular velocities.
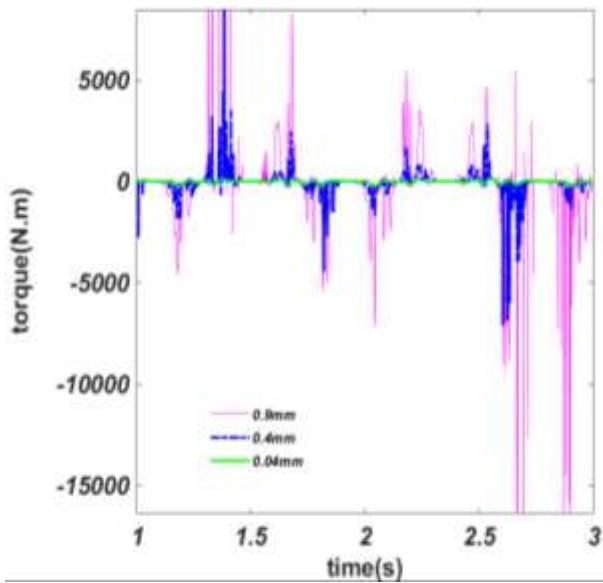
Fig. 15   Crank moment for different clearance sizes.

In this part, two cases are examined. In the first case, a four-bar linkage mechanism with one clearance joint between links 3 and 4 (i) (according to "Fig. 4"), and in the second case (ii) a four-bar linkage mechanism with a clearance joint between links 3 and 4 and a compliant joint between link 2 and 3 (according to "Fig. 5") are considered. Figure 16 shows dynamic behaviour of the second case in several stiffness. The yellow curves of "Figs. 16c and 16d" illustrate that the sudden changes of

acceleration and moment curves are decreased by applying the compliant joint and this causes the enhancement in the useful life and dynamic behaviour of the system. According to "Fig. 16", the compliant joint with k=4 shows better behaviour than the case of k=10. These figures show that by optimizing the stiffness of compliant joint, the acceleration curve is improved. However, by other stiffness far away from the region of proportional stiffness, the behaviour of mechanism is not improved impressively. Although the sudden change of acceleration and severe collision in clearance joint is not canceled, the behaviour of mechanism via optimized compliant joint stiffness is improved by decreasing impact in clearance joint and maximum acceleration amplitude of linkages.

(a)

(b)

(c)

(d)
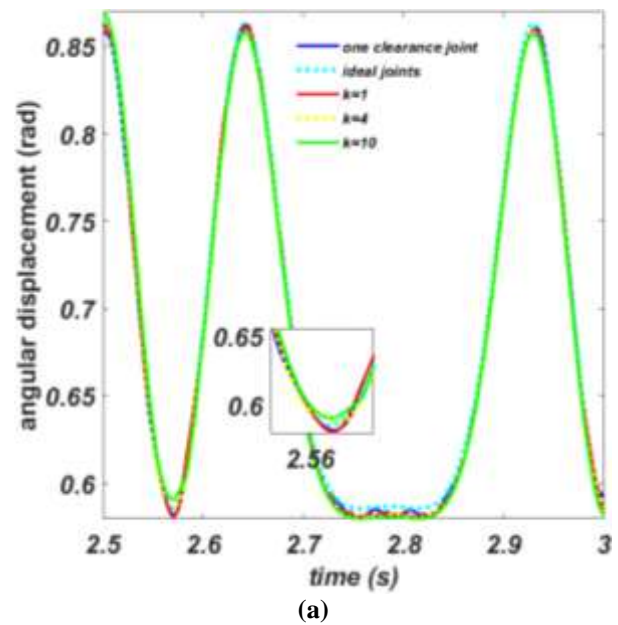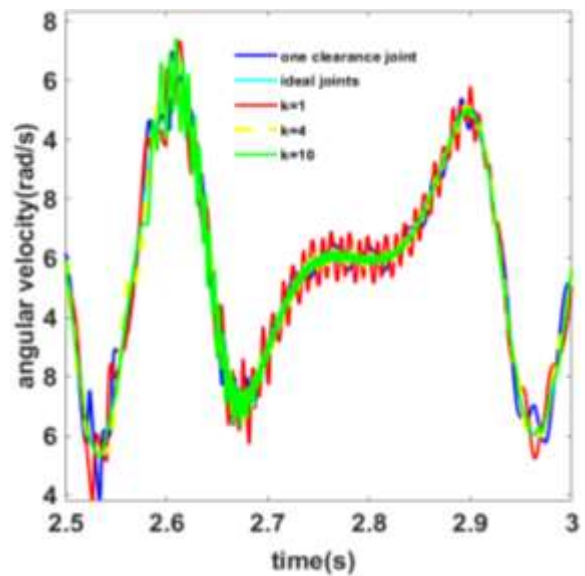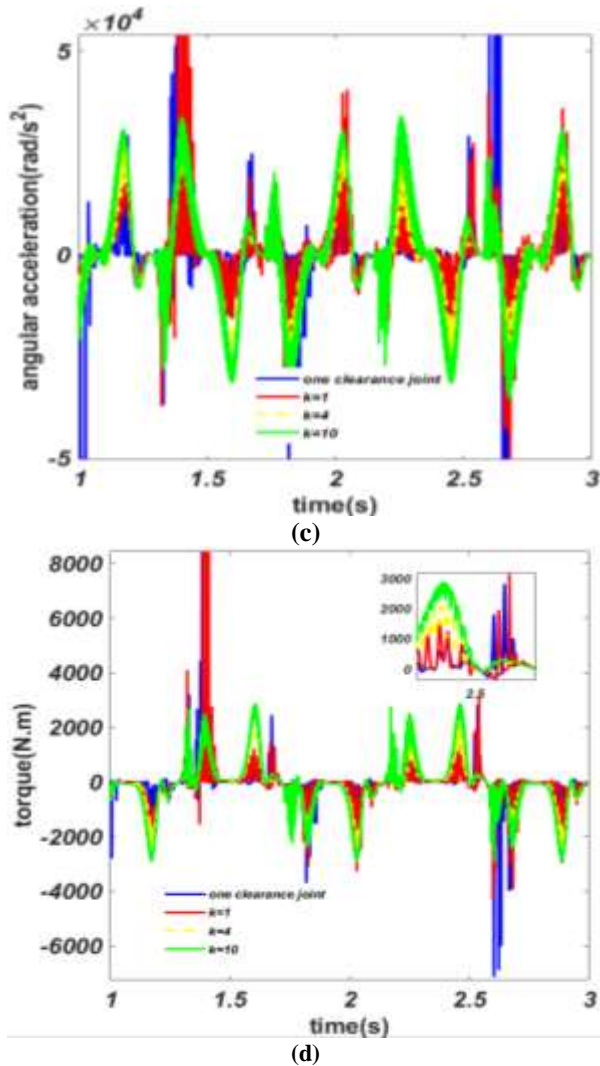
Fig. 16 Angular position, velocity and acceleration of the coupler of case (ii): (a): couple angle displacement, (b): couple velocity, (c): couple acceleration, (d): input torque.

According to previous sections, there are some parameters that affect the clearance in joints like the stiffness of joint, clearance size, and input link velocity. The present study focuses on the effect of compliant joint stiffness. Moreover one of the important ways to improve clearance influence on the vibration of mechanism is selecting the optimized stiffness of compliant joint. Therefore, in this section based on a number of impacts in the clearance joint the stiffness of the compliant joint is optimized. Figure 17 shows the number of impacts in the clearance joint according to the stiffness of the compliant joint. This figure demonstrated the range of stiffness for minimum impact. Therefore, the advantage of this figure is used to optimize the compliant joint in order to eliminate the undesirable vibration of the mechanism with clearance joint. Subsequently, the nonlinear dynamics of the mechanism are investigated in the following section.
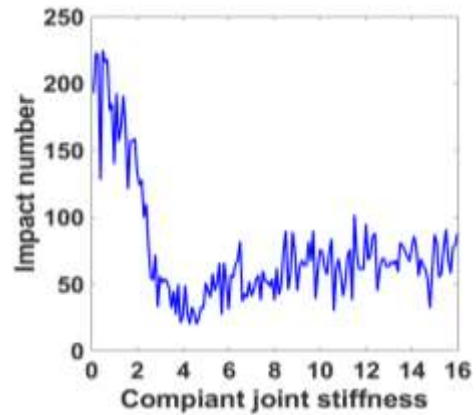
Fig. 17 Impact number versus compliant joint stiffness.

Figyre 18 shows the crank moment in the two mentioned cases. The sudden changes appeared in "Fig. 18" are because of the impact existed in the clearance joint. Figure 16 clearly illustrates that the dynamic behaviour of the system with clearance joint will be improved by using the compliant joint with proper bending coefficient. Figure 18 shows that by using the compliant joint, the clearance joint experiences fewer free flight and impact modes, therefore, the impact of the system and the sudden changes of the moment curve are decreased.
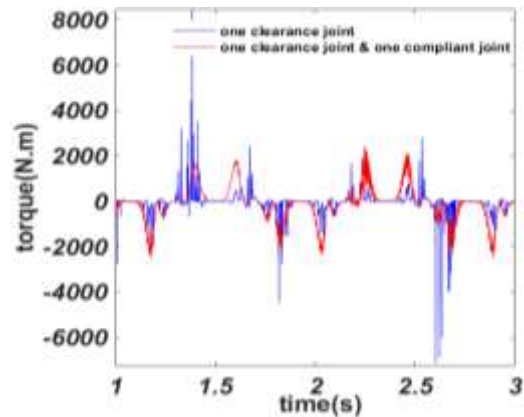
Fig. 18 Crank Moment of case (i) and (ii).

Table 4 The comparative numerical results

Considering case	Number of impact	Follower maximum acceleration	Maximum contact force
4-bar linkage with one clearance	207	2.053×10^5	9988
4-bar linkage with one clearance and one compliant joint	33	2.57×10^4	3587

Consequently, the system performance is improved and the useful life of the system is increased. As a quantitative result, applying optimized compliant joint, 84% of impacts, 87% of follower maximum acceleration, and 64% of Maximum contact force are decreased. "Table. 4" shows the comparative numerical results. The phase diagram is the graph that is commonly used for nonlinear vibration analysis. Figure 19 demonstrates the phase diagram of the ideal mechanism and the two mentioned cases for both 6 cycles (0s-5.16s) and one cycle (1.93s-2.79s). There are undesirable changes in the plots of the two mentioned cases, because of clearance. However, this phenomenon is not seen in ideal mechanism plots.
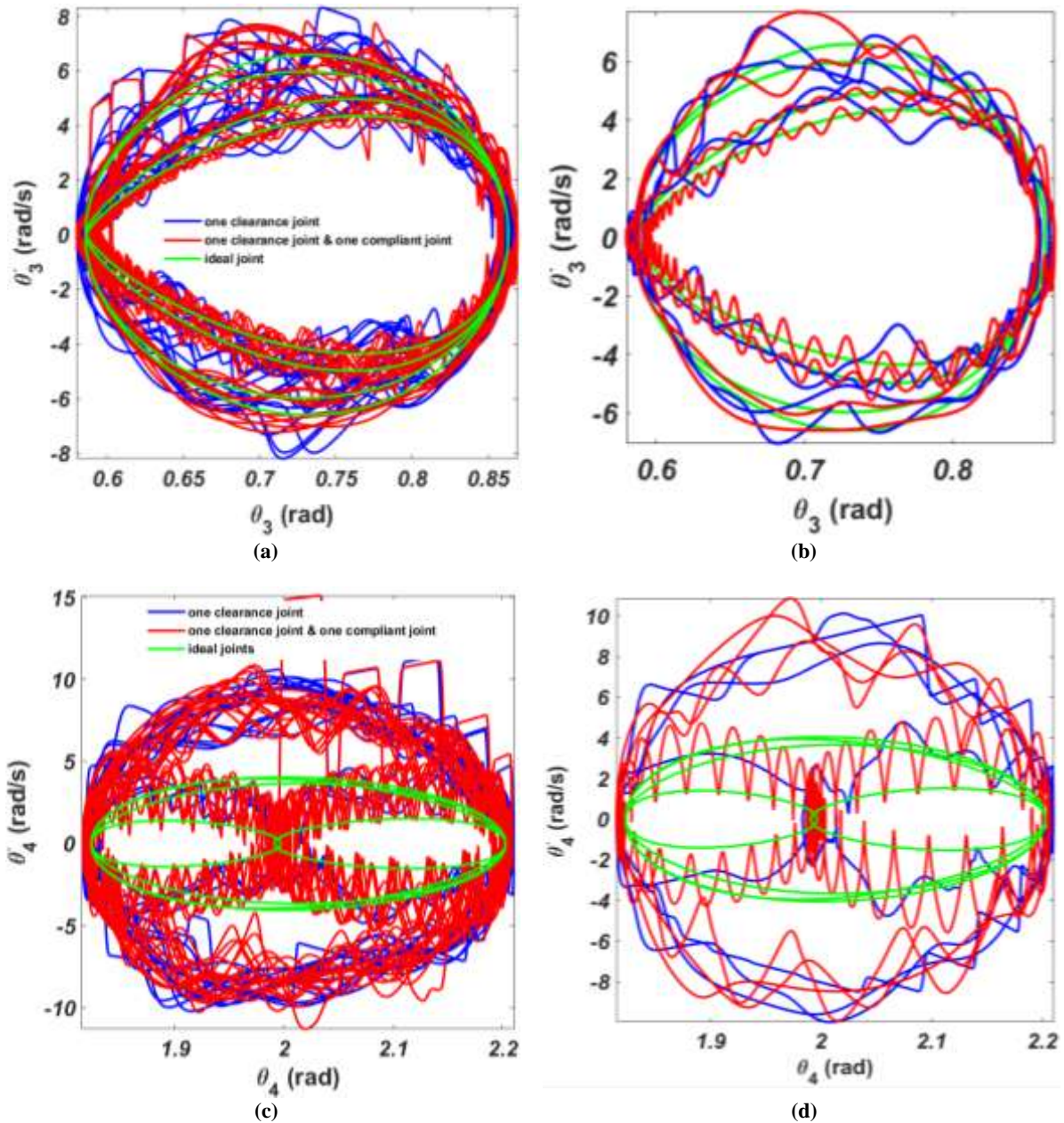
Fig. 19   Phase diagram: (a):$\theta_3 - \dot{\theta}_3$, (b): $\theta_3 - \dot{\theta}_3$ for one cycle, (c): $\theta_4 - \dot{\theta}_4$, (d): $\theta_4 - \dot{\theta}_4$ for one cycle.

Figure 20 shows the Poincare section for cases (i) and (ii). Nonlinear behaviour of these cases because of clearance is proved, since if the Poincare section of the system does not include finite discrete points; nonlinear system behaviour will be likely [10]. By comparing the two cases, it is evident that the system with a complaint joint has less chaotic behaviour given its fewer and finite discrete points.

Figure 21 shows the Poincare section based on the coupler's velocity in terms of clearance size for the two mentioned cases. This figure suggests that the number of discrete points increases with the increase in the clearance size, which in turn leads to a more chaotic system. By conducting a comparison between "Fig. 21a and 21b", the number of Poincare points in "Fig. 21b" is lower than that of "Fig. 21a", hence, the system in the state shown in "Fig. 21b" has less nonlinear behaviour in comparison to "Fig. 21a".
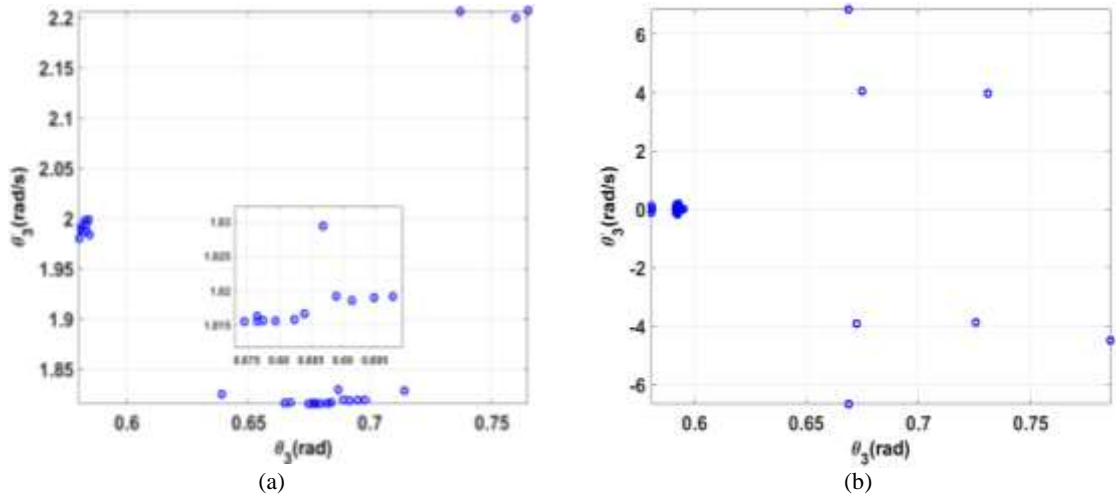
Fig. 20 Bifurcation diagram of mechanism for clearance size $C = 0.4$, for: (a): clearance joint of 3, and (b): clearance joint 3 with compliant joint 2 for stiffness of k=4.
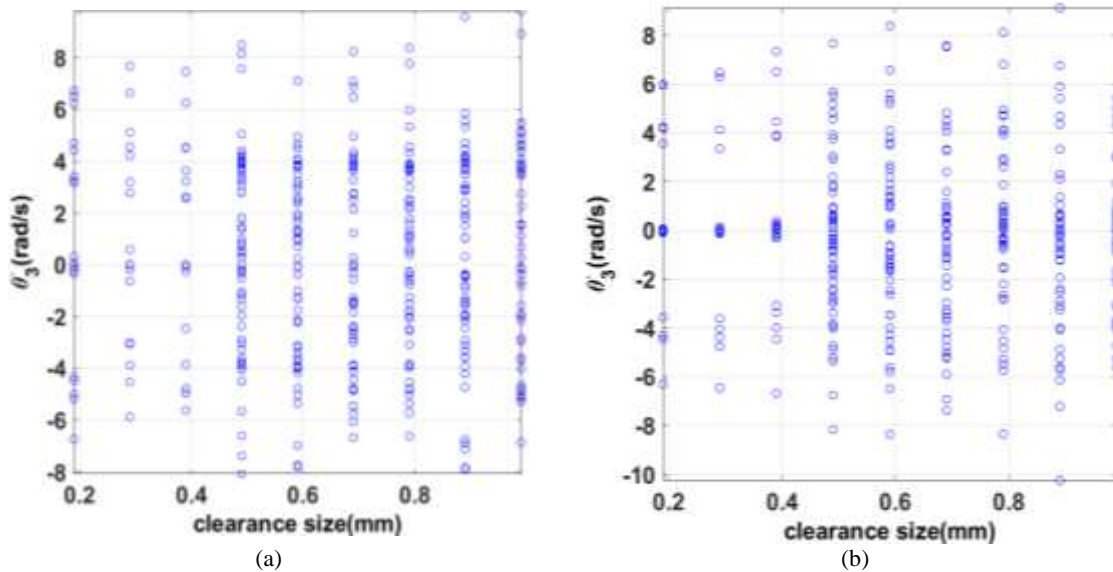
Fig. 21 Poincare map for angular velocity of coupler for different clearance size: (a): with one clearance joint, (b): with one clearance and one compliant joint.

Figure 22 gives the FFT analysis of the coupler's velocity for cases (i) and (ii) for different compliant joint stiffness. The number of frequencies in the mechanism with a compliant joint is fewer than that of the mechanism with only one clearance joint, leading to fewer vibrations in the mechanism with a compliant joint, while the amplitude of these vibrations is larger. Therefore, the compliant joint improves the system behaviour and reduces undesirable vibrations. As can be seen, the number of frequencies in the mechanism with a compliant joint is fewer when comparing the optimized stiffness case to others. However, the amplitude of vibration is larger for this case. Figure 23 shows the phase diagram, it can be concluded for optimized compliant joint stiffness that the curve of the phase diagram is smoother.
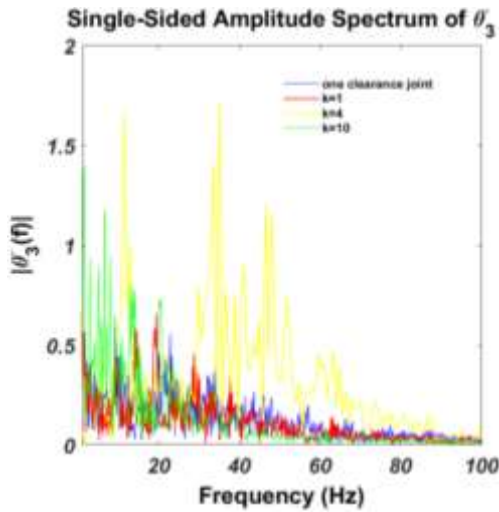
Fig. 22 Power spectrum of $\dot{\theta}_3$ of case (i) and (ii) with different stiffness of compliant joint.
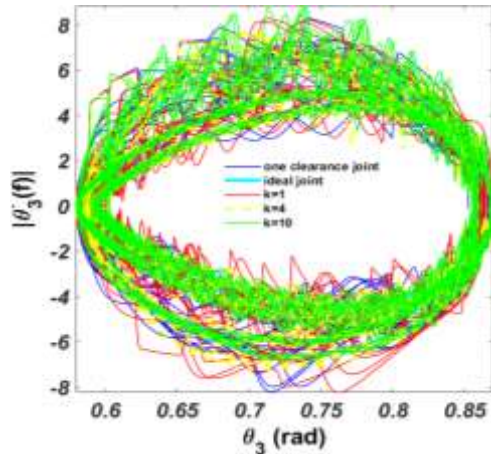
Fig. 23 Phase diagram ($\theta_3 - \dot{\theta}_3$) of case (ii) for several compliant joint stiffness.
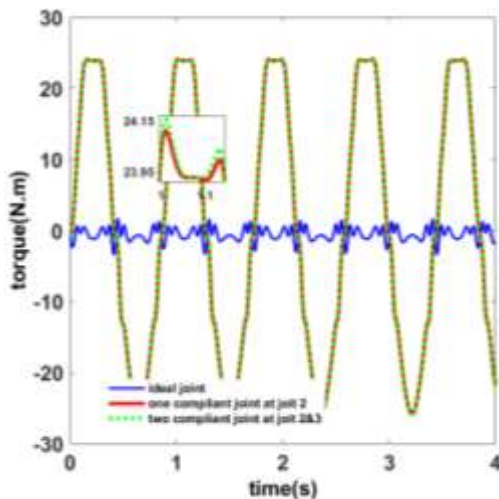
Fig. 24 Crank moment of four bar linkage mechanism with one compliant joint at joint 2 and four bar linkage mechanism with two compliant joint at joint 2 and 3.

A four-bar mechanism with two compliant joints according to "Fig. 24" is considered. The required moment for the movement of the input link in the mechanism with compliant joints is larger than the ideal one; however, this value is significantly lower compared to that of the mechanism with the clearance joint. Therefore, although compliant joints increase the required moment but the advantages of them in mechanism with clearance joint is preferable. Moreover, it is noteworthy that increasing the number of compliant joints in the system increases the value of the required input moment.

4 CONCLUSION

The main goal of this paper is to examine the influence of compliant joints on the nonlinear dynamics of mechanisms with the clearance joint. Lagrange Equations are used to derive EoM, and Lankarani-Nikravesh model is used for contact force calculation. Considering the addition of a clearance joint to a four-bar linkage mechanism with one DoF, three DoFs are obtained, and since the compliant joint is assumed a torsion spring, no change in the number of DoF occurs. Moreover, the Runge-Kutta 4th order method is applied to solve EoM.

The results reveal the significant efficiency of applying a compliant joint for reducing undesirable vibration due to the clearance joint. Furthermore, the outcome of increasing input link velocity and clearance size is the increase of undesirable system vibrations.

Moreover, present research represented that by using a proper bending compliant joint, an improved dynamical behaviour can be achieved. So by concentrating on the bending stiffness of a compliant joint, dimensions of this joint are selected in order to improve dynamical behaviour. The simulation of the mechanism in 6 cycles demonstrates the 207 impacts in clearance joint for mechanism without compliant joint, however compliant joint decreases impacts to 33, the follower maximum acceleration is $2.053 \times 10^5 (\frac{rad}{s^2})$ for the mechanism without compliant joint, however compliant joint decreases follower maximum acceleration to 2.57×10^4, and the maximum contact force in clearance joint is 9988 for the mechanism without compliant joint, however compliant joint decreases maximum contact force to 3587. According to the quantitative results, the compliant joint can increase the life of mechanisms with the clearance joint. Moreover, examining nonlinear behaviour analysis confirmed our conclusion.

Apparently, there are some limitations in our proposed model in terms of considering axial stiffness and translation of compliant joint, and lubrication effect in clearance joint to achieve more accurate models.

However, the suggestion can be extended by considering the 3D vector of clearance radius to simulate 3D mechanisms and robotic systems to eliminate the undesirable effect of clearance joint by using compliant joint.

REFERENCES

[1]   Seneviratne, L. D., Earles S. W., and Fenner D. N., Analysis of a Four-Bar Mechanism with a Radially Compliant Clearance Joint, Proceedings of the Institution of Mechanical Engineers, Part C: Journal of Mechanical Engineering Science. Vol. 210, No. 3, 1996, pp. 215-223, DOI: 10.1243%2FPIME_PROC_1996_210_191_02.

[2]   Chen, Y., Feng J., Peng, X., Sun, Y., He, Q., and Yu, C., An Approach for Dynamic Analysis of Planar Multibody Systems with Revolute Clearance Joints, Engineering with Computers, Vol. 37, No. 3, 2021, pp. 2159-2172, DOI: 10.1007/s00366-020-00935-x.

[3]   Lankarani, H. M., Nikravesh, P. E., A Contact Force Model with Hysteresis Damping for Impact Analysis of Multibody Systems, In International Design Engineering Technical Conferences and Computers and Information in Engineering Conference, Vol. 3691, pp. 45-51. American Society of Mechanical Engineers, DOI: 10.1115/1.2912617.

[4]   Pereira C. M., Ramalho A. L., and Ambrósio J. A., A Critical Overview of Internal and External Cylinder Contact Force Models, Nonlinear Dynamics, Vol. 63, No. 4, 2011, pp. 681-697, DOI: 10.1007/s11071-010-9830-3.

[5]   Flores, P., Ambrósio, J., Claro, J. C. P., Lankarani, H. M., and Koshy, C. S, A Mechanism and Machine Theory, Vol. 41, No. 3, 2006, pp. 247-261, DOI: 10.1016/j.mechmachtheory.2005.10.002.

[6]   Koshy, C. S., Sony, Ch., Flores, P., and Lankarani, H. M., Study of the Effect of Contact Force Model on The Dynamic Response of Mechanical Systems with Dry Clearance Joints: Computational and Experimental Approaches, Nonlinear Dynamics, Vol. 73, No. 1, 2013, pp. 325-338, DOI: 10.1007/s11071-013-0787-x.

[7]   Varedi, S. M., Bamdad, M., The Effects of Joint Clearance on the Dynamics of the 3-RPR Planar Parallel Manipulator, Advance Design and manufacturing Technology, Vol. 11, No. 2, 2018, pp. 120-113, DOI: 10.1017/S0263574715001095.

[8]   Ebrahimi, S., Salahshoor, E., and Nouri, S., Sensitivity Analysis for Optimal Design of Multibody Systems with Clearance Joint, Advance Design and Manufacturing Technology, Vol. 11, No. 3, 2018, pp. 35-44, ISSN: 2252-0406.

[9]   Flores, P., Koshy, C. S., Lankarani, H. M., Ambrósio, J., and Koshy, C. S., Numerical and Experimental Investigation on Multibody Systems with Revolute Clearance Joints, Nonlinear Dynamics, Vol. 65, No. 4, 2011, pp. 383-398, DOI: 10.1007/s11071-010-9899-8.

[10] Javanfar, A., Daniali, H. M., Dardel, M., and Ghasemi, M. H., Dynamic Behaviour Analysis of Four-Bar Linkage Mechanisms with Joints' Clearance, In 2015 3rd RSI International Conference on Robotics and Mechatronics (ICROM), pp. 383-388, IEEE, 2015, DOI: 10.1109/ICRoM.2015.7367815.

[11] Javanfar, A., Bamdad, M., Effect of Novel Continuous Friction Model on Nonlinear Dynamics of The Mechanisms with Clearance Joint, Proceedings of the Institution of Mechanical Engineers, Part C: Journal of Mechanical Engineering Science (2021), Vol. 236, No. 11, 2022, pp. 6040-6052, DOI: 10.1177%2F09544062211063432.

[12] Marques, F., Flores, P., Pimenta, C., and Lankarani, H. M., A Survey and Comparison of Several Friction Force Models for Dynamic Analysis of Multibody Mechanical Systems, Nonlinear Dynamics, Vol. 86, No. 3, 2016, pp. 1407-1443, DOI: 10.1007/s11071-016-2999-3.

[13] Azimi-Olyaei, A., Ghazavi, M. R, Stabilizing Slider-Crank Mechanism with Clearance Joints, Mechanism and Machine Theory, Vol. 53, 2012, pp. 17-29, DOI: 10.1016/j.mechmachtheory.2012.02.006.

[14] Yaqubi, S., Dardel, M., Daniali, H. M., and Ghasemi, M. H., Modeling and Control of Crank–Slider Mechanism with Multiple Clearance Joints, Multibody System Dynamics, Vol. 36, No. 2, 2016, pp. 143-167, DOI: 10.1007/s11044-015-9486-3.

[15] Erkaya, S., Uzmay I., Investigation on Effect of Joint Clearance on Dynamics of Four-Bar Mechanism, Nonlinear Dynamics, Vol. 58, No. 1, 2009, pp. 179-198, DOI: 10.1007/s11071-009-9470-7.

[16] Sardashti, A., Daniali H. M., and Varedi S. M., Optimal Free-Defect Synthesis of Four-Bar Linkage with Joint Clearance Using PSO Algorithm, Meccanica, Vol. 48, No. 7, 2013, pp. 1681-1693, DOI: 10.1007/s11012-013-9699-6.

[17] Varedi, S. M., Daniali, H. M., Dardel, M., and Fathi, A., Optimal Dynamic Design of a Planar Slider-Crank Mechanism with a Joint Clearance, Mechanism and Machine Theory, Vol. 86, 2015, pp. 191-200, DOI: 10.1007/s11012-013-9699-6.

[18] Bai, Z. F., Zhao, Y., A Hybrid Contact Force Model of Revolute Joint with Clearance for Planar Mechanical Systems, International Journal of Non-Linear Mechanics, Vol. 48, 2013, pp. 15-36, DOI: 10.1016/j.ijnonlinmec.2012.07.00.

[19] Liu, X., Ding, J., and Wang, C., Design Framework for Motion Generation of Planar Four-Bar Linkage Considering Clearance Joints and Dynamics Performance, Machines, Vol. 10, No. 2, 2022, pp. 136, DOI: 10.3390/machines10020136.

[20] Hua, G., Jingyu, Z., Hao, Z., Qingkai, H., and Jinguo, L., Dynamic Investigation of a Spatial Multi-Body Mechanism Considering Joint Clearance and Friction Based on Coordinate Partitioning Method, Proceedings of the Institution of Mechanical Engineers, Part C: Journal of Mechanical Engineering Science, Vol. 235, No. 24, 2021, pp. 7569-7587, DOI: 10.1177%2F09544062211025566.

[21] Yaqubi, S, Dardel, M, and Daniali, H. M., Nonlinear Dynamics and Control of Crank–Slider Mechanism with Link Flexibility and Joint Clearance, Proceedings of the Institution of Mechanical Engineers, Part C: Journal of Mechanical Engineering Science, vol. 230, no. 5, 2016, pp. 737-755, DOI: 10.1177%2F0954406215593773.

[22] Erkaya, S., Doğan, S., and Şefkatlıoğlu, E., Analysis of the Joint Clearance Effects on a Compliant Spatial Mechanism, Mechanism and Machine Theory, Vol. 104, 2016, pp. 255-273, DOI: 10.1016/j.mechmachtheory.2016.06.009.

[23] Oh, Y. S., Kota, S., Synthesis of Multistable Equilibrium Compliant Mechanisms Using Combinations of Bistable Mechanisms, Journal of Mechanical Design, Vol. 131, No. 2, 2009, DOI: 10.1115/1.3013316.

[24] Erkaya, S., Effects of Joint Clearance on the Motion Accuracy of Robotic Manipulators, Strojniski Vestnik/Journal of Mechanical Engineering, Vol. 64, No. 2, 2018, DOI: 10.5545/sv-jme.2017.4534.

[25] Amiri, A., Dardel, M., and Daniali, H. M., Effects of Passive Vibration Absorbers on The Mechanisms Having Clearance Joints, Multibody System Dynamics, Vol. 47, No. 4, 2019, pp. 363-395, DOI: 10.1007/s11044-019-09684-2.

[26] Moon, Y. M., Trease, B. P., and Kota, S., Design of Large-Displacement Compliant Joints, InInternational Design Engineering Technical Conferences and Computers and Information in Engineering Conference, Vol. 36533, 2002, pp. 65-76, American Society of Mechanical Engineers, DOI: 10.1115/DETC2002/MECH-34207" \t.

[27] Fowler, R. M., Maselli, A., Pluimers, P, Spencer P. M., and Howell, L. L., Flex-16: A Large-Displacement Monolithic Compliant Rotational Hinge, Mechanism and Machine Theory, Vol. 82, 2014, pp. 203-217, DOI: 10.1016/j.mechmachtheory.2014.08.008.

[28] Wang, N., Xiaohe, L., and Xianmin, Z., Pseudo-Rigid-Body Model for Corrugated Cantilever Beam Used in Compliant Mechanisms, Chinese Journal of Mechanical Engineering, Vol. 27, No. 1, 2014, pp. 122-129, DOI: 10.3901/CJME.2014.01.122.

[29] Li, Z., Tsagarakis, N. G., and Caldwell, D. G., Walking Pattern Generation for a Humanoid Robot with Compliant Joints, Autonomous Robots, Vol. 35, No. 1, 2013, pp. 1-14, DOI: 10.1007/s10514-013-9330-7.

[30] Timoshenko, S., History of Strength of Materials: with a Brief Account of The History of Theory of Elasticity and Theory of Structures, Courier Corporation, 1983, ISBN: 0486611876.

[31] Ugwuoke, I. C., Abolarin, M. S., and Ogwuagwu, O. V., Dynamic Behaviour of Compliant Slider Mechanism using the Pseudo-Rigid-Body Modeling Technique, AU JT, Vol. 12, No. 4, 2009, pp. 227-234.